

Performance evaluation of geosynthetic reinforced flexible pavement using full-scale accelerated loading tests

Murad Abu-Farsakh¹ and Shadi Hanandeh²

¹ Research Professor, Louisiana Transportation Research Center, Louisiana State University, Baton Rouge, LA 70808. (Corresponding author).

² Assistant Professor, Department of Civil Engineering, Balqa Applied University, Amman, Jordan.

ABSTRACT

An accelerated traffic load testing was conducted on full-scale test lane sections to evaluate the benefits of using geogrids to enhance the performance of pavement constructed over soft subgrade. Six full-scale test lane sections were constructed, among which two sections were reinforced by one or two layers of triaxial geogrids, two sections were reinforced by one layer of high strength geotextile with different base layer thickness, and the remaining two sections were the control sections. The test sections were instrumented by a variety of sensors to measure the load- and environment-associated pavement response and performance. Results of the full-scale testing on the pavement test sections demonstrate the benefits of using geosynthetics in reducing the permanent deformation in the pavement structure. The benefit of geosynthetics on the resilient properties of pavement is more distinguishable at higher load level. It was also found that the geosynthetic placed at the base-subgrade interface was able to improve the performance of both subgrade and base layers; by placing an additional layer of geogrid at the upper one-third of the base layer, the performance of base layer was further enhanced.

INTRODUCTION

In the state of Louisiana, roads often have to be built over a weak subgrade due to the soft nature of Louisiana soil and the presence of high ground water table, which creates many design and construction challenges. Cement or lime is commonly used to treat weak subgrade soil in Louisiana to create a working platform layer. However, geosynthetics can offer a potentially economical and environment friendly alternative solution for stabilizing roads built over weak subgrade soil. The concept of using geosynthetics as reinforcement in roadway construction started in the 1970s. Since then, numerous studies have revealed that using geosynthetic reinforcements in pavement structures either extends the pavement service life and/or reduces the base layer thickness (e.g., Tingle and Jersey 2005; Chen et al. 2009; Perkins et al. 2009; Abu-Farsakh and Chen 2011; Jersey et al. 2012; Tang et al. 2013). The geosynthetic type, the location/layers of geosynthetics, the base thickness, and the subgrade strength have significant effect on the performance of geosynthetic reinforced flexible pavement (e.g., Perkins 1999; Al-Qadi et al. 2008). With the pavement design moving toward Mechanistic-Empirical (ME) based methods (e.g., AASHTO Pavement ME), recent studies on geosynthetic applications in pavements have been focused on quantifying the effects and benefits of geosynthetics and incorporating them into the ME analysis and design (e.g., Perkins et al. 2009; Chen and Abu-Farsakh 2012). To this end, the pavement responses and performance under cyclic loading have often been monitored with a variety of sensors.

OBJECTIVES

The main objective of this research is to evaluate the benefits of using geosynthetics to reinforce base layer and/or stabilize weak subgrade soil in flexible pavement application. For this purpose, six field moving wheel load tests were conducted. A variety of sensors were installed for each section to measure load-and environment- associated pavement response and performance, which could be used to quantify the benefits of using geosynthetics within the framework of Mechanistic Empirical Pavement Design Guide (MEPDG).

TESTING PROGRAM

Test Sections and Instrumentation

Six test lane sections were constructed over native soft soil. The test sections were 24 m (80 ft) long and 4 m (13 ft) wide. The cross sections of the six test lanes are depicted in Figure 1. Section 1 was constructed over a 305 mm thick sand embankment wrapped by nonwoven geotextile as a common practice in Southern Louisiana. Section 2 and Section 3 were reinforced/stabilized by the triaxial geogrid placed at the base-subgrade interface. An additional layer of geogrid reinforcement was also installed at the upper one-third of the base layer thickness in Section 3. Section 4 is the control section that was constructed without geosynthetic reinforcement. The high strength geotextiles were used to reinforce/stabilize Section 5 and Section 6 with different base layer thicknesses. A 76-mm HMA surface course was constructed over the test lane sections.

The test sections were instrumented by a variety of instruments to measure the load – and environment – associated pavement responses and performance. Figure 2 depicts a typical layout of instrumentations used in this study. For each test section, two earth pressure cells (Geokon Model 3500) were installed at the top of the subgrade to measure the total vertical stresses. Piezometers (Geokon Model 3400) were installed next to the pressure cells to measure possible excess pore water pressure generated by the cyclic wheel load. Spring-loaded LVDTs (RDP DCTH2000A) were customized to measure the total deformation of the subgrade. Potentiometers (Honeywell MLT-38000201) were customized to measure the strain at the mid-height of the aggregate layer.

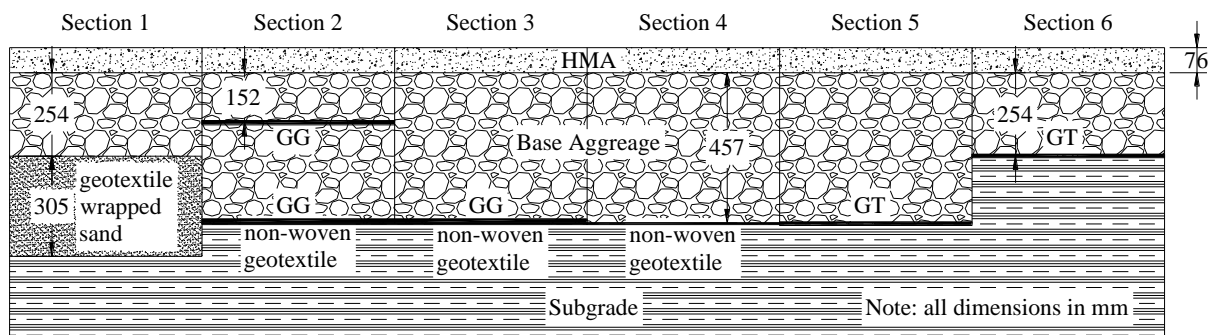


Figure 1 Cross section of pavement test sections

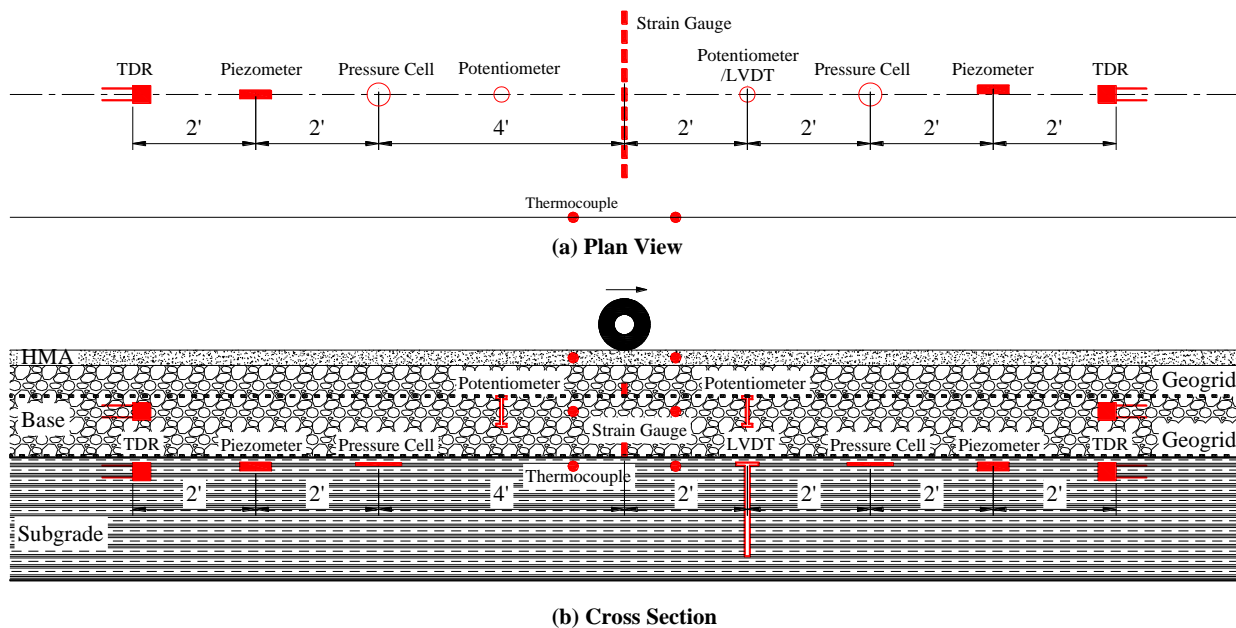


Figure 2 Instrumentation plan for test section 2

Pavement Layer Materials

Subgrade. The native subgrade soil consisted of a high plasticity clay, having a liquid limit of 88 and a plastic index of 53 with 96.6 % passing # 200. It is classified as CH per Unified Soil Classification System (USCS) or A-7-6 according to the American Association of State Highway and Transportation Officials (AASHTO) classification system. The clay has an optimum moisture content of 35% and a maximum dry density of 1,250 kg/m³ according to the standard Proctor test.

Base Course Material. Mexican crushed limestone material was used in the base course layer for all test sections. The crushed limestone had 1.56% passing No. 200 opening sieve, an effective particle size (D_{10}) of 0.382 mm, a mean particle size (D_{50}) of 3.126 mm, a D85 of 19 mm, a uniformity coefficient (C_u) of 37, and a coefficient of curvature (C_c) of 3. This crushed limestone is classified as GW and A-1-a according to the USCS and the AASHTO classification systems, respectively. The maximum dry density, as determined by the modified Proctor test is 2,066 kg/m³ at an optimum moisture content of 9.4%.

HMA Concrete. The HMA used in the construction is a wearing course. It is a 12.5 mm design level 1 Superpave mixture. The asphalt binder was classified as PG 76-22M according to the Performance Grade (PG) specification. The optimum asphalt binder content is 4.1%. The theoretical maximum density of HMA is 2,480 kg/m³.

Geosynthetics. Two types of geosynthetics were used in this research, a Triaxial geogrid, GG, and a high-strength woven geotextile, GT. The physical and mechanical properties of these geosynthetics as provided by the manufacture are presented in Table 1.

Table 1 Physical and mechanical properties of geosynthetics used in this study

Reinforcement	Polymer Type	T, kN/m		J, kN/m		Aperture Size, mm
		MD ^a	CD ^b	MD ^a	CD ^b	
GG	Polypropylene	1.35 ^c		270 ^d		40×40×40
GT	Polypropylene	7.0 ^e	26.3 ^e	350 ^f	1313 ^f	0.425 ^g

^aMachine direction, ^bCross machine direction, ^cTensile strength at 0.5% strain in radial direction, ^dTensile modulus at 0.5% strain in the radial direction, ^eTensile strength at 2% strain, ^fTensile modulus at 2% strain, ^gApparent opening size (AOS)

Test Facilities

A full-scale accelerated load facility (ALF) was used to apply rolling wheel loads on the test lane sections. Figure 3 shows a picture of the ALF with an insert of the dual-wheel assembly. ALF is a testing device that applies unidirectional trafficking to the test sections with a nominal speed of 16.8 km/h (10.5 mph) or 350 passes per hour. ALF has a dual-tire axle consisting of two Michelin XZE-model truck tires. The load is adjustable from 43.4 kN (9,750 lb) to 84.4 kN (18,950 lb). With a computer-controlled load trolley, the weight and movement of traffic is simulated in one direction at a speed of 10.5 mph (16.8 km/h). Lateral wander normally distributed over a width of 762 mm (30 in) [381 mm (30 in) at each side of the pavement centerline] was considered in this experiment. The wheel path generated by ALF is about 12 m (40 ft).

The test was conducted in two phases for all sections: (1) pre-rut loading phase, prior to construction of HMA layer, and (2) main loading phase, after HMA construction. During the pre-rut phase, the applied load was 43.4 kN (9,750 lb). The base course were pre-rutted to a maximum rut depth of 25 mm (1") or 2000 passes, whichever comes first, prior to HMA paving. The discussions of the results of the pre-rut loading phase can be found in Tang et al. (2015). This paper focuses on the results of main loading phase. During the main loading phase, the sections is loaded to 19 mm (¾") rut depth. The starting load was 43.4 kN (9,750 lb). The load was increased to 53.6 kN (12,050 lb) after 110,000 cycles (151,510 ESALs), and then to 63.8 kN (14,350 lb) after 210,000 cycles (472,860 ESALs). The tire pressure was set to 724 kPa (105 psi).



Figure 3 Rolling wheel load testing facility

TEST RESULTS

Resilient Responses under Moving Traffic Load

The pavement resilient responses to moving traffic load are of great importance because they can be used to calibrate and verify the mechanistic models for ME analysis and design. Figure 4a

shows the vertical stresses at the top of subgrade layer as measured by the pressure cells. Figure 4b shows the peak vertical stress at the top of subgrade at different stages of traffic loading for all the test sections. In general, the vertical stresses on top of the subgrade remained a relatively stable state throughout the testing. As expected, Section 6 registered the highest pressure due to shallow depth of subgrade layer while Section 1 registered lowest pressure due to deeper subgrade layer, compared to the other sections. The difference in magnitudes of the peak subgrade stress between unreinforced (Section 4) and reinforced (Sections 2, 3, and 5) sections is not significant when the applied load is 43.4 kN (9,750 lb), indicating that geosynthetics may have limited contribution to the resilient properties of pavement at this load level. With the increase of load, however, the benefit of geosynthetics on the resilient properties of pavement becomes more distinguishable.

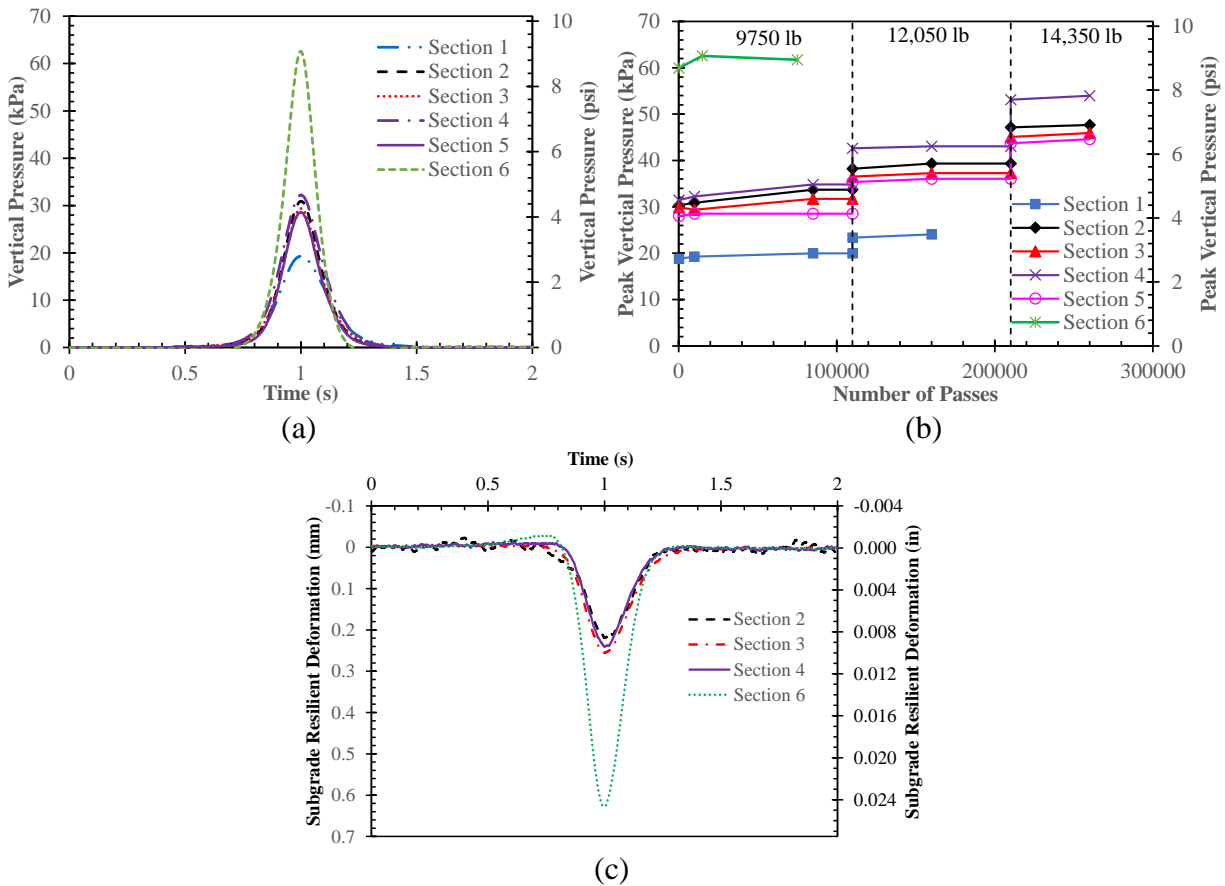


Figure 4 Resilient responses: (a) transient vertical subgrade stress at wheel pass of 10,000; (b) peak subgrade vertical stress along with number of wheel passes; (c) resilient subgrade deformation at wheel pass of 10,000

Surface Permanent Deformation

Figure 5 presents the accumulation of the total permanent deformation along with the number of EASLs for the six test lane sections. The total permanent deformation for each test lane section shown in Figure 5 is the average of the measurements taken at the six different locations along the wheel path in each section. The results show that sections constructed with geosynthetics

experienced less rut depth than the control section. As compared to the single layer geogrid reinforcement section, more reduction in the pavement surface deformation was observed for the double layer geogrid reinforcement section (Section 2).

In addition to the presence of geosynthetics, other factors can affect the performance of the test sections in resisting the surface rutting. Although efforts were made to ensure consistent or similar in-situ conditions for all test sections, variations in construction, such as material placing and degree of compaction, may affect the section performance. The change of the subgrade soil and aggregate layer conditions throughout the testing process may also affect the sections' performance. Noticeably, there was a drastic increase in surface rutting after 1,119,165 ESALs for section 2 and 796,012 ESALs for section 3. This sudden increase in surface rutting is believed to be related to the heavy rainfall occurred during that period and the design drainage system could not handle that amount of rain. The DCP data showed that the bottom one-third of base material was significantly weakened, with DCPI increased from around 10 mm/blow to around 50 mm/blow. This clearly demonstrates the significant importance of drainage in the performance of pavement structure, both reinforced and unreinforced sections. The AASHTO Pavement ME was utilized by the authors to simulate the weakening effect of the bottom of base layer by dividing the base layer of sections 2 and 3 into two layers (upper strong base and bottom weak base). The permanent deformations were then adjusted by assuming the bottom weak base having the same property as the upper strong base. The adjusted permanent deformation curves were also presented in Figure 5. It can be seen from the figure that Sections 2, 3 and 5 can sustain 1,405,861, 1,280,429 and 1,652,365 ESALs at a rut depth of 19 mm (3/4") which result a traffic benefit ratio (TBR) of 1.53, 1.40, and 1.80, respectively. The TBR is defined as the number of load cycles carried by a reinforced section at a specific rut depth divided by that of an equivalent unreinforced section.

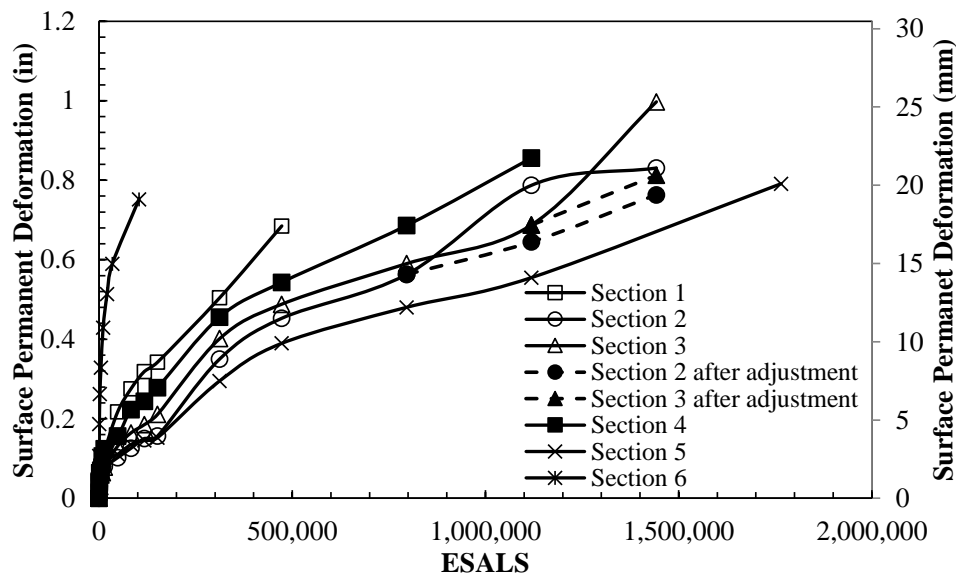


Figure 5 Accumulated total permanent deformation

Permanent Deformation in Subgrade and Base

As previously mentioned, the customized potentiometer was installed at the mid-height of base layer to estimate the overall deformation of the base layer. The overall deformation of the

subgrade layer was measured by a customized LVDT. Figures 6a and b illustrate the development of subgrade and base permanent deformation with number of ESALS. As can be seen from the figures, for the control section (Section 4), the base layer makes more significant contribution to the total permanent deformation, when compared to the subgrade layer. The use of geosynthetics resulted in reducing the permanent deformations in both the base and subgrade layers (Sections 2 and 3). Compared with Section 3, Section 2, with two layers of geogrids, showed similar reduction of permanent deformation in subgrade layer but noticeably less aggregate layer deformation. This suggests that while the performance of base and subgrade was improved by the geogrid at the base-subgrade interface, the performance of base layer was further enhanced by the geogrid placed at the upper one-third of the base layer.

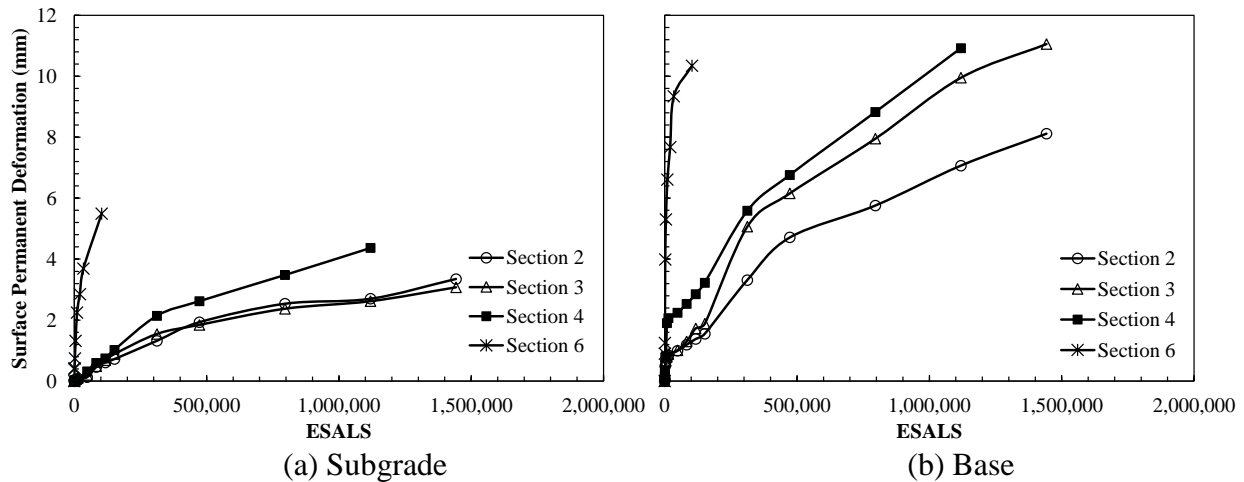


Figure 6 Accumulated permanent deformation in subgrade and base layer

CONCLUSION

An accelerated traffic load testing was conducted on full-scale test lane sections to evaluate the benefits of using geosynthetics to reinforce/stabilize aggregate layer/subgrade in paved roads. A total of six test lane sections were constructed over native soft subgrade soil, and were extensively instrumented to measure the critical pavement responses and performance.

Results of the full-scale accelerated load testing demonstrated the benefits of geosynthetics in significantly reducing the total permanent deformation/surface rutting of pavement test sections. The benefits of geosynthetics on the resilient properties of pavement are more distinguishable at the higher load level. Instrumentation measurements indicate that the base layer makes more significant contribution to the total permanent deformation than the subgrade layer. The deformation in the aggregate layer is most likely due to further compaction and densification of the layer. While geosynthetics placed at base-subgrade interface is able to improve the performance of both subgrade and base layers. By placing an additional layer of geogrid at the upper one-third of the base layer, the performance of base layer is further enhanced. With the inclusion of geosynthetic reinforcement, the TBR can be increased up to 1.8 at a rut depth of 19 mm for pavement constructed using 457 mm (18 in.) thick base layer on top of weak subgrade soil. The drainage has important effect on the performance of pavement structures, both unreinforced and reinforced sections.

ACKNOWLEDGEMENTS

The authors acknowledge and appreciate the financial support provided by the Louisiana Department of Transportation and Development (LA DOTD), Tensar International., and TenCate. The authors also wish to thank the personnel at Pavement Research Facility of Louisiana Transportation Research Center (LTRC) and the graduate students at LTRC who helped with installing instruments and in-situ testing.

REFERENCES

- Abu-Farsakh, M. and Chen, Q. (2011). Evaluation of Geogrid Base Reinforcement in Flexible Pavement Using Cyclic Plate Load Testing, *International Journal of Pavement Engineering*, Vol. 12 Issue 275-288.
- Al-Qadi, I.L., Dessouky, S.H., Kwon, J., and Tutumluer, E. (2008). Geogrid in flexible pavements: validated mechanism. *Transportation Research Record: Journal of Transportation Research Board 2045*, pp. 102-109.
- Chen, Q. and Abu-Farsakh, M. (2012) Structural Contribution of Geogrid Reinforcement in Pavement. *GeoCongress 2012*.1468-1475.
- Chen, Q., Abu-Farsakh, M., and Tao, M. (2009). Laboratory evaluation of geogrid base reinforcement and corresponding instrumentation program. *Geotechnical Testing Journal*, ASTM, Vol. 32, No.6, pp. 516-525.
- Jersey, S. R., Tingle, J. S., Norwood, G. J., Kwon, J., and Wayne, M. (2012). “Full-Scale Evaluation of Geogrid-Reinforced Thin Flexible Pavements.” *Transportation Research Record 2310*, Transportation Research Board, National Research Council, Washington, D.C.: 61–71.
- Perkins, S.W. (1999). Geosynthetic Reinforcement of Flexible Pavements Laboratory Based Pavement Test Sections. Federal Highway Administration Report *FHWA/MT-99-001/8138*, Montana Department of Transportation, Helena, Montana, USA, 109
- Perkins, S.W., Christopher B.R., Cuelho, E.G., Eiksund, G. R., Schwartz, C.S., and Svanø, G. (2009). A Mechanistic-Empirical Model for Base-Reinforced Flexible Pavements,” *International Journal of Pavement Engineering*, Vol. 10, No. 2, 101–114.
- Tang, X., Abu-Farsakh, M., Hanandeh, S., Chen, Q. 2015. “Performance of Reinforced and Stabilized Unpaved Test Sections Built over Native Soft Soil under Full-Scale Moving Wheel Loads” *Transportation Research Record: Journal of the Transportation Research Board, National Research Council*.
- Tang, X., Stoffels, S. M., and Palomino, A. M. (2013). “Resilient and Permanent Deformation Characteristics of Unbound Pavement Layers Modified by Geogrids.” *Transportation Research Record 2369*, Transportation Research Board, National Research Council, Washington, D.C.: 3–10.
- Tingle, J. and Jersey, S. (2005). Cyclic Plate Load Testing of Geosynthetic-Reinforced Unbound Aggregate Roads *Transportation Research Record: Journal of the Transportation Research Board, No. 1936*, Transportation Research Board of the National Academies, Washington, D.C., 2005, 60–69.